Original Article

Progressive changes in non-neoplastic ground-glass nodules on follow-up computed tomography (CT)

Jin Jiang[1#], Ting-Wei Xiong[1,2#], Bin-Jie Fu[1], Wang-Jia Li[1], Rui-Yu Lin[1], Fa-Jin Lv[1*], Zhi-Gang Chu[1*^]

[1]Department of Radiology, The First Affiliated Hospital of Chongqing Medical University, Chongqing, China; [2]Department of Radiology, The Second Affiliated Hospital of Army Medical University, Chongqing, China

Contributions: (I) Conception and design: ZG Chu, FJ Lv; (II) Administrative support: ZG Chu; (III) Provision of study materials or patients: J Jiang, TW Xiong; (IV) Collection and assembly of data: J Jiang, TW Xiong, WJ Li, RY Lin; (V) Data analysis and interpretation: J Jiang, TW Xiong, BJ Fu; (VI) Manuscript writing: All authors; (VII) Final approval of manuscript: All authors.

[#]These authors contributed equally to this work.

[*]These authors contributed equally to this work as corresponding authors.

Correspondence to: Fa-Jin Lv, MD, PhD; Zhi-Gang Chu, MD, PhD. Department of Radiology, The First Affiliated Hospital of Chongqing Medical University, 1# Youyi Road, Yuanjiagang, Yuzhong District, Chongqing 400016, China. Email: 1779848907@qq.com; chuzg0815@163.com.

Background: Non-neoplastic ground-glass nodules (GGNs) generally decrease in size or density during follow-up; however, some exhibit the opposite effect (and show progressive changes), which can lead to unnecessary resection. This study sought to determine the progressive changes in non-neoplastic GGNs using follow-up computed tomography (CT).

Methods: This cross-sectional study included 70 patients diagnosed with pathologically confirmed non-neoplastic GGNs from January 2017 to March 2023. Of the patients, 35 showed progressive changes and 35 showed no significant changes. The initial and preoperative chest CT images were reviewed to evaluate their changes. The progressive changes in the GGNs were classified into the following five types: type I: increasing density; type II: increasing size; type III: increasing density and solid component; type IV: increasing size and density/solid component; and type V: increasing size, density, and solid component. The T-test, Pearson chi-square test, Wilkinson sign test and Mann-Whitney U-test were used for the data analysis. A two-sided P value <0.05 was considered statistically significant.

Results: Among the 35 GGNs with progressive changes, type II (14, 40.0%) was the most common, followed by types IV (9, 25.7%), I (5, 14.3%), V (5, 14.3%), and III (2, 5.3%). The number of lesions that changed in <6, ≥6 and <12, ≥12 and ≤24, >24 months was 22 (62.9%), 4 (11.4%), 5 (14.3%), and 4 (11.4%), respectively. Among the 28 GGNs with an increasing volume, the number of lesions with a volume doubling time (VDT) of <344 and >441 days was 20 (71.4%) and 8 (28.6%), respectively. Except for these progressive changes, the other features did not exhibit significant changes, especially the ill-defined boundary (74.3% *vs.* 71.4%, P>0.99).

Conclusions: GGNs with progressive changes are more likely to be non-neoplastic if the changes occur in a short period or the lesions maintain an ill-defined boundary.

^ ORCID: 0000-0003-4016-7270.

Introduction

With the popularization of lung cancer screening, and the application of thin-section computed tomography (TSCT), the detection of pulmonary nodules, especially ground-glass nodules (GGNs), has dramatically increased (1). GGNs can be divided into pure ground-glass nodules (pGGNs) and part-solid nodules (PSNs) based on the presence of solid components in the lung window (2). Pathologically, GGNs can be caused by various non-neoplastic disorders or neoplastic lesions. The former include inflammation, edema, fibrosis, and hemorrhage, while the latter usually include atypical adenomatous hyperplasia, adenocarcinoma *in situ*, minimally invasive adenocarcinoma, and invasive adenocarcinoma (3-6). Clinically, the treatments for neoplastic and non-neoplastic GGNs differ significantly. Consequently, it is necessary to distinguish between neoplastic and non-neoplastic GGNs for subsequent clinical decision making.

The qualitative diagnosis of GGNs largely depends on the display of their detailed manifestations on TSCT. Previous studies have discussed the imaging features that suggest neoplastic and non-neoplastic GGNs in detail (7-13). Generally, nodules with a larger size, well-defined boundary, the vascular convergence sign, lobulation, spiculation, pleural traction, and irregular or scattered solid components are highly suggestive of neoplastic lesions, while those with an irregular shape or ill-defined boundary are usually considered non-neoplastic (7-13). However, there is some overlap between the morphological characteristics of neoplastic and non-neoplastic GGNs, which makes their differential diagnosis more complex. Therefore, in addition to evaluating the computed tomography (CT) features, follow-up of indeterminate GGNs may provide additional important information for further diagnosis (2,14-16).

The follow-up recommendations were determined based on the risk of malignancy of incidental lung nodules, which is related to the nodule size, shape, attenuation, etc. Nodule size remains the primary factor for determining the likelihood of malignancy (14). For GGNs ≥6 mm, routine follow-up is recommended. Specifically, GGNs that are ≥6 mm should be followed-up for 5 years, and can considered benign if they resolve or decrease in size or density based on the current guidelines (2,15). Conversely, a progressive increase in the overall size or the size of internal solid components, the occurrence of solid components, or persistent PSNs with solid components ≥6 mm are highly indicative of neoplasms (2,16).

In clinical practice, neoplastic GGNs typically exhibit an increase in size and/or density during follow-up; however, some non-neoplastic GGNs may also exhibit changes that could be seen as "progressive changes" in contrast to traditional changing trends. Non-neoplastic GGNs with progressive changes can be easily misdiagnosed, leading to unnecessary resection. However, there have been no relevant reports describing the characteristics of non-neoplastic GGNs with progressive changes and how to distinguish them from neoplastic ones. Thus, this study sought to retrospectively investigate the data of patients with non-neoplastic GGNs with progressive changes from two centers, and identify the key characteristics of them. We present this article in accordance with the STROBE reporting checklist (available at https://qims.amegroups.com/article/view/10.21037/qims-24-389/rc).

Methods

Patient selection

The study was conducted in accordance with the Declaration of Helsinki (as revised in 2013), and the study protocol was approved by the ethics committees of The First Affiliated Hospital of Chongqing Medical University (No. 2019-062) and The Second Affiliated Hospital of Army Medical University (No. 2020-research147-01). The requirement of written informed consent was waived due to the retrospective nature of the study. All the personal identification data were anonymized and de-identified before analysis.

The electronic health records (EHRs) of The First Affiliated Hospital of Chongqing Medical University and The Second Affiliated Hospital of Army Medical University

were searched to identify patients who underwent resection of a pulmonary lesion by the thoracic surgery service from January 2017 to March 2023. In total, 4,101 patients with benign lesions were identified. The preoperative chest CT images of these patients were manually reviewed on the Picture Archiving and Communication System (PACS) (version 3.1.S19.5, Carestream Vue, Carestream), after which 817 patients were excluded because the resected pulmonary lesions were not nodules (567 were patches and 250 were masses), and 2,460 patients were excluded because the lesions were solid nodules rather than GGNs. A pulmonary nodule was defined as a rounded, oval, or irregular opacity, well or poorly defined, measuring up to 3 cm in diameter (17). A GGN was a radiological finding showing a hazy opacity with the presence of the underlying pulmonary vessels or bronchial structures in high-resolution CT (17). Ultimately, the data of 824 patients with 824 pathologically confirmed non-neoplastic GGNs were preliminarily collected. Among these patients, 567 were excluded due to the absence of repeated CT data (552 patients) or thin-section CT data (15 patients). Based on the initial and repeated CT images, the changes in density, size (diameter and volume), and internal solid component of the remaining 257 GGNs were evaluated.

The changes in the GGNs were classified into the following two types: (I) progressive changes: increases in the size, density and/or solid component during follow-up; and (II) non-neoplastic changes: disappearance of GGNs or decreasing in the size, density, and/or solid component during follow-up. Size increasing was defined as an increase in the maximal diameter of ≥2 mm, or an increase in volume of at least 25% (18,19). In the present study, the volume change of lesions was used to evaluate the size change. Density increasing was defined as an increase in the CT value of ≥100 HU. Solid component increasing was defined as an increase of at least 1.5 mm in the solid-component mean diameter, an increase of at least 25% in the volume, or the occurrence of new solid components (18,19). GGNs without progressive changes and non-neoplastic changes were classified as having no significant changes.

After comparisons, GGNs in 14 patients showed a slight decrease in solid components (9 patients) or size (5 patients), GGNs in 208 patients exhibited no significant changes, and 35 GGNs in 35 patients showed a size, density, and/or solid component increase. For comparison with the GGNs with progressive changes, we selected all the GGNs with a follow-up time >6 months from 208 cases of GGNs without significant changes. Ultimately, 35 GGNs with progressive

changes and 35 GGNs with no significant changes were enrolled in the study. The patient selection procedure is shown in *Figure 1*.

CT protocol

The chest CT scans were performed using one of the following scanners: SOMATOM Perspective, SOMATOM Definition Flash, or SOMATOM Force (Siemens Healthineers, Erlangen, Germany). Scans were obtained with the patient at full inspiration to minimize breathing artifacts. Changes in GGNs were evaluated based on the non-enhanced CT images. All the non-contrast chest CT images were acquired with the following settings: tube voltage: 100–130 kVp; tube current time: 40–140 mAs (using automatic current modulation technology); scanning slice thickness: 5 mm; rotation time: 0.5 s; pitch, 1–1.1; collimation: 0.6 or 0.625 mm; reconstruction slice thickness and interval, 0.625 or 1 mm; and matrix: 512×512. Images were obtained with mediastinal (width, 350–400 HU; level, 20–40 HU) and lung (width, 1,200–1,600 HU; level, –500 to –700 HU) window settings. All the GGNs were evaluated in the lung window.

Clinical data and image analysis

The patients' clinical data were obtained using the Electronic Medical Record System (Winning Health, China). Clinical data, including patients' age, sex, smoking history, clinical symptoms, underlying disease, history of malignant tumor, and family history of lung cancer, were collected. The CT data were independently reviewed by two radiologists (J.J. and T.W.X. with 3 and 8 years of experience in chest CT interpretation, respectively) on a PACS workstation (version 3.1.S19.5, Carestream Vue, Carestream). Any discrepancy in the findings between the two radiologists was resolved by consensus. The preliminary results were confirmed by another senior radiologist (Z.G.C. with 16 years of experience in chest CT interpretation).

The following CT features of the GGNs were analyzed: (I) size (the average of the longest diameter and the perpendicular diameter on axial images); (II) shape (round, oval, or irregular); (III) distribution (upper, middle, or lower lobe); (IV) CT pattern (pGGN or PSN); (V) mean CT value; (VI) volume; (VII) volume doubling time (VDT); (VIII) boundary (well-defined or ill-defined); and (IX) other morphological features (lobulation, spiculation, vacuole sign, pleural indentation, and air bronchogram). The mean
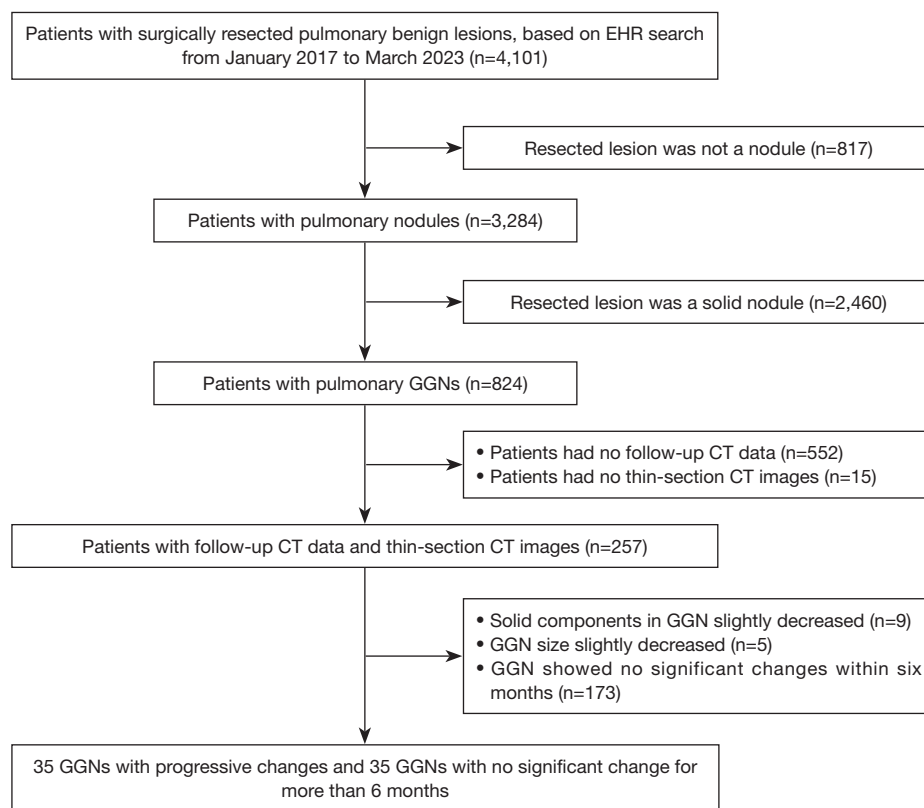
Figure 1 Flowchart of study population. EHR, electronic health record; GGN, ground-glass nodule; CT, computed tomography.

CT value was measured three times on TSCT using a region-of-interest cursor to calculate the mean value and measurement areas covering two-thirds of the largest area in the GGN while avoiding vessels and bronchioles (20). The volume of each GGN was measured using artificial intelligence software (InferRead CT Lung, InferVision Medical Health, China). VDT was calculated as follows: $VDT = (t \times \log 2)/[\log (V_t/V_0)]$, where V_t and V_0 are the volume of the GGN at the latest preoperative and initial TSCT scan, respectively, "t" is the interval between these two CT scans, $\log (V_t/V_0)$ is the log to the base 10 of (V_t/V_0), and $\log 2$ is the log to the base 10 of 2 (21). The progressive changes in the GGNs were classified into the following five types in this study: type I: increasing density (*Figure 2*); type II: increasing volume (*Figure 3*); type III: increasing density and solid component (*Figure 4*); type IV: increasing volume and density/solid component; and type V: increasing volume, density, and solid component. Based on these types of progressive changes, group 1 included GGNs with changes of types I and III, and group 2 included those with changes of types II, IV, and V, respectively.

Pathological analysis

The pathological findings of the non-neoplastic GGNs included fibrous tissue proliferation and/or inflammatory cell infiltration, fibroblast and myofibroblast hyperplasia, and hyaline degeneration. The non-neoplastic nodules were classified into two groups based on their main pathological findings: (I) fibrous tissue proliferation with inflammatory cell infiltration; and (II) fibrous tissue proliferation without inflammatory cell infiltration.

Statistical analysis

The statistical analysis was performed using SPSS (version 26.0, IBM, NY, USA). The continuous data are expressed as the mean ± standard deviation, or the median ± interquartile range, while the categorical variables are expressed as the number and percentage. The normality test was used to examine differences in size, volume, and density between the groups. If the data were normally distributed, the paired *t*-test or *t*-test was used; otherwise, the Wilkinson sign test
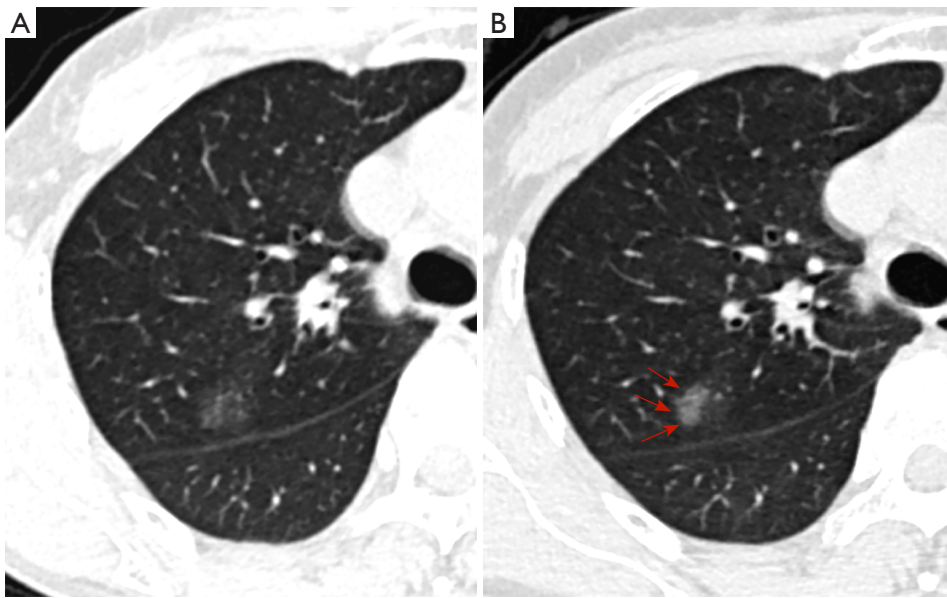
Figure 2 A 54-year-old female with an incidental GGN. (A) An axial CT image showed a 13.4-mm round and ill-defined pGGN with a mean density of –668 HU located in the right upper lobe. (B) A follow-up CT scan performed 6.7 months later showed an increase in density (–493 HU) (red arrows). The histopathologic analysis revealed fibrous tissue proliferation with less inflammatory cell infiltration. GGNs, ground-glass nodules; CT, computed tomography; pGGN, pure ground-glass nodule; HU, Hounsfield unit.
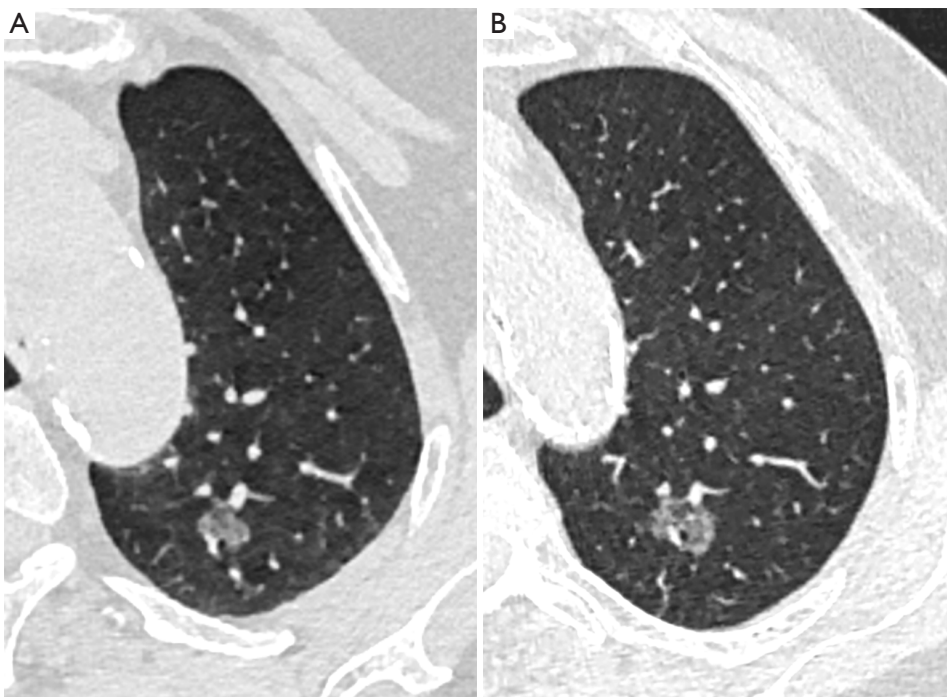

Figure 3 An 80-year-old female with an incidental GGN. (A) An axial CT image showed a 14-mm round and well-defined PSN with a volume of 667 mm^3 located in the left upper lobe. (B) A follow-up CT scan performed 13 months later showed an increase in volume (2,003 mm^3). The histopathologic analysis revealed fibrous tissue proliferation with less inflammatory cell infiltration. GGN, ground-glass nodule; CT, computed tomography; PSN, part-solid nodule.
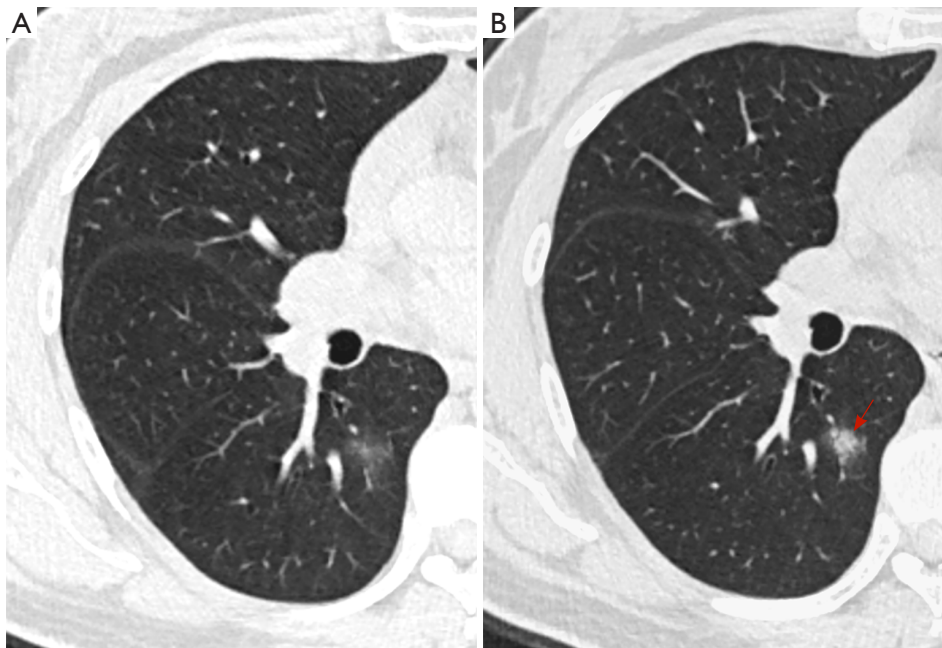
Figure 4 A 52-year-old female with an incidental GGN. (A) An axial CT image showed a 14-mm round and ill-defined pGGN with a mean density of –609 HU located in the right lower lobe. (B) A follow-up CT scan performed 27 days later showed an increase in density (–324 HU) and the development of new solid components (red arrow). The histopathologic analysis revealed fibrous tissue proliferation with less inflammatory cell infiltration. GGN, ground-glass nodule; CT, computed tomography; pGGN, pure ground-glass nodule; HU, Hounsfield unit.

or Mann-Whitney U-test was used. A Pearson chi-square test was used to compare the CT features of the GGNs on the initial and latest preoperative images, as well as the main pathological findings between GGNs with progressive changes and those without any significant changes for >6 months. A two-sided P value <0.05 was considered statistically significant.

Results

Clinical characteristics of patients

Among the 35 patients with non-neoplastic GGNs showing progressive changes (mean age: 54.9±10.5 years; range, 34–80 years), 18 (51.4%) were female and 17 (48.6%) were male. Nine (25.7%) of these patients were smokers, and 7 (20.0%), 17 (48.6%), 2 (5.7%), and 2 (5.7%) had respiratory symptoms, underlying diseases (diabetes, hyperthyroidism, and chronic obstructive pulmonary disease, and pulmonary tuberculosis), a history of malignant tumor, and a family history of lung cancer, respectively. Among the 35 patients with non-neoplastic GGNs showing

no significant changes (mean age: 51.9±11.8 years; range, 30–75 years), 20 (57.1%) were female and 15 (42.9%) were male. Five (14.3%) of these patients were smokers, and 9 (25.7%), 4 (11.4%), 0 (0.0%), and 5 (14.3%) had respiratory symptoms, underlying disease, a history of malignant tumor, and a family history of lung cancer, respectively. With the exception of underlying diseases, there were no significant differences between the GGN patients with and without progressive changes in terms of age, sex, smoking history, respiratory symptoms, history of malignant tumor, and a family history of lung cancer (P=0.001).

CT characteristics of the GGNs on the initial and latest preoperative CT images

The CT characteristics of the GGNs on the initial and latest preoperative CT images are set out in Tables 1,2. Among the 35 GGNs with progressive changes, the number of lesions that changed in <6, 6–12, 12–24, and >24 months was 22 (62.9%), 4 (11.4%), 5 (14.3%), and 4 (11.4%), respectively. In addition, the boundary of 5 (14.3%) and 4 (11.4%) lesions changed from ill-defined to well-defined,

Table 1 CT characteristics of the GGNs with progressive changes on the initial and latest preoperative CT images

Characteristics	Initial CT scan (n=35)	Latest preoperative CT scan (n=35)	P value
Size (mm)	9.90±4.41	11.76±6.03	–
CT value (HU)	−539.66±171.95	−437.29±220.05	–
Volume (mm³)	758.90±1,170.98	1,380.52±2,705.68	–
Distribution			–
Upper and middle lobe	21 (60.0)	21 (60.0)	
Lower lobe	14 (40.0)	14 (40.0)	
CT pattern			0.81[†]
Pure GGN	18 (51.4)	16 (45.7)	
PSN	17 (48.6)	19 (54.3)	
Shape			>0.99[†]
Regular	27 (77.1)	27 (77.1)	
Irregular	8 (22.9)	8 (22.9)	
Boundary			>0.99[†]
Ill-defined	26 (74.3)	25 (71.4)	
Well-defined	9 (25.7)	10 (28.6)	
GGNs with other signs	9 (25.7)	13 (37.1)	0.057[†]
Lobulation	4 (44.4)	6 (46.2)	
Spiculation	1 (11.1)	1 (7.7)	
Vacuole sign	1 (11.1)	1 (7.7)	
Bronchial cut-off	2 (22.2)	2 (15.4)	
Air bronchogram	1 (11.1)	2 (15.4)	
Pleural indentation sign	0	1 (7.7)	

Data are presented as n (%) or mean ± standard deviation. [†], calculated with the Pearson Chi-squared test. – indicated no statistical data. CT, computed tomography; GGNs, ground-glass nodules; HU, Hounsfield unit; PSN, part-solid nodules.

and from well-defined to ill-defined, respectively. Among the 35 GGNs without changes, the boundary of 2 (5.7%) lesions changed from well-defined to ill-defined. The initial CT features of the progressive GGNs and those without changes were compared, and no significant differences were found in terms of the CT pattern, shape, and boundary, but the GGNs with progressive changes had a greater initial diameter (P=0.04).

Progressive changes in GGNs

The groups of progressive changes on the initial and latest preoperative CT images are detailed in *Table 3*. Among the 35 GGNs with progressive changes, type II (14, 40.0%) was the most common, followed by types IV (9, 25.7%), I (5, 14.3%), V (5, 14.3%), and II (2, 5.3%). In groups 1, the density of the GGNs were significantly higher or larger on the latest preoperative CT images than the initial CT images (P<0.05). In groups 2, the diameter, volume and density of the GGNs were significantly higher or larger on the latest preoperative CT images than the initial CT images (P<0.05). The follow-up intervals for the GGNs in group1 were similar to those for group 2 (42.0±263.0 *vs.* 144.0±281.0, P=0.16).

GGNs with increasing volumes

There were significant differences in the size, volume,

Table 2 CT characteristics of the GGNs without changes on the initial and latest preoperative CT images

Characteristics	Initial CT scan (n=35)	Latest preoperative CT scan (n=35)	P value
Size (mm)	7.80±3.12	7.93±2.90	–
CT value (HU)	−560.88±152.53	−569.38±154.93	–
Distribution			–
Upper and middle lobe	27 (77.1)	27 (77.1)	
Lower lobe	8 (22.9)	8 (22.9)	
CT pattern			>0.99[†]
Pure GGN	19 (54.3)	19 (54.3)	
PSN	16 (45.7)	16 (45.7)	
Shape			–
Regular	35 (100)	35 (100)	
Irregular	0 (0)	0 (0)	
Boundary			0.49[†]
Ill-defined	33 (94.3)	35 (100)	
Well-defined	2 (5.7)	0 (0)	
GGNs with other signs	2 (5.7)	2 (5.7)	>0.99[†]
Spiculation	1 (50.0)	1 (50.0)	
Vacuole sign	1 (50.0)	1 (50.0.)	

Data are presented as n (%) or mean ± standard deviation. [†], calculated with the Pearson Chi-squared test. – indicates no statistical data. CT, computed tomography; GGNs, ground-glass nodules; HU, Hounsfield unit; PSN, part-solid nodules.

and density among the nodules with the same CT pattern on the initial and latest preoperative CT images (pGGN, P<0.001; PSN, P<0.05). The initial and latest preoperative density of the PSNs were significantly higher than those of the pGGNs (−461.62±117.56 *vs.* −663.60±79.79 HU, −338.31±190.85 *vs.* −607.80±119.70 HU) (P<0.001), but there were no significant differences in the other features of different CT patterns in the initial and latest preoperative CT images (P>0.05). Among the 28 (80%) (15 pGGNs and 13 PSNs) with increasing volume, the number of lesions with a VDT of <344 and >441 days was 20 (71.4%), 8 (28.6%), respectively. The VDTs of the total lesions, pGGNs, and PSNs were 501.8±840.6 (range, 43.6–3,415.3), 545.1±807.5 (range, 57.2–3,015.8), and 451.9±907.9 (range, 43.6–3,415.3) days, respectively. The VDTs of the pGGNs and PSNs were similar (P=0.47).

Pathological findings for GGNs with and without progressive changes

The main pathological findings for the GGNs with progressive changes and those without changes beyond 6 months are listed in *Table 4*. The more common pathological findings included fibrous tissue proliferation with inflammatory cell infiltration, but there was no significant difference between the GGNs with progressive changes and those without changes (P=0.79). In nine cases of progressive GGNs with boundary changes, the pathological results of seven cases were fibrous tissue proliferation with inflammatory cell infiltration, and the pathological results of the remaining cases were fibrous tissue proliferation without inflammatory cell infiltration. In the two cases of stable GGNs with boundary changes, the pathological results showed fibrous tissue proliferation with inflammatory cell infiltration.

Discussion

Compared with neoplastic GGNs, non-neoplastic GGNs generally disappearing, decreasing in size or density, or stably persist for at least five years during follow-up (2,15).

Table 3 The groups of the GGNs with progressive changes on the initial and latest preoperative CT images

Characteristics	Group 1	Group 2
Numbers (n=35)	7 (20.0)	28 (80.0)
Follow-up interval (days)	42.0 [263.0]	44.0 [281.0]
Diameter (mm)		
Initial	9.5±4.9	10.5 [5.2]
Follow-up	9.5±4.9	11.7 [5.0]
P value	>0.99[‡]	<0.001[†]
Volume (mm³)		
Initial	217.5±1,014.1	559.0 [645.0]
Follow-up	253.1 [1,391.5]	976.5 [944.2]
P value	0.13[†]	<0.001[†]
VDT (days)	–	167.9 [368.3]
Density (HU)		
Initial	−526.0±178.8	569.8 ±141.3
Follow-up	−255.7±189.0	−482.7±205.8
P value	0.003[‡]	0.001[‡]

Data are presented as n (%), or mean ± standard deviation, or median [interquartile range]. [†], calculated with the Wilkinson sign test; [‡], calculated with the paired *t*-test. Group 1 includes GGNs with changes of type I and III; Group 2 includes GGNs with changes of type II, IV, and V. – indicates no statistical data. GGNs, ground-glass nodules; CT, computed tomography; VDT, volume doubling time; HU, Hounsfield unit.

In the present study, some non-neoplastic GGNs (13.6%) showed various progressive changes (an increase in the volume, density, and/or solid component) in both the short- and long-term follow-up periods. Except for these progressive changes, the other morphological features of the lesions did not show significant changes, especially the boundary, which was mainly ill-defined both on the initial and latest preoperative CT images. As the non-neoplastic GGNs can show similar changes to the neoplastic GGNs during follow-up, they are more likely to be misdiagnosed, and thus further differentiation is necessary.

The progressive changes of non-neoplastic and neoplastic GGNs are similar, but their pathological analyses differ significantly. The non-neoplastic GGNs showed more or less inflammatory cell infiltration and fibrous tissue proliferation, while the neoplastic GGNs showed tumor cell growth. It may be that changes in non-neoplastic lesions are related to inflammation and its stage. In the early stage, the infiltration and exudation of inflammatory cells increase as the lesions progress. Over time, inflammation subsides and reaches an advanced stage with fibrous tissue proliferation. As a result, follow-up CT scans can capture increases in the size, density, and solid component in some lesions at different stages. These changes can be detected in both short- and long-term follow-up. The former may be due to GGNs being in the early stage of inflammation on initial detection, while the latter may be related to the patient suffering chronic inflammation due to the influence of the natural environment, food safety, or stress, or the GGNs might have changed before the follow-up, but those changes might not have been detected in time, resulting in an increase in the follow-up period. Thus, the initial manifestation of lesions and the interval of follow-up may be related to their different changes.

No follow-up is required for a single subsolid nodule <6 mm, regardless of whether it is a pGGN or PSN. While follow-up scanning is recommended at 6–12 months for solitary pGGNs ≥6 mm, and at 3–6 months for solitary PSNs ≥6 mm (2,14,15). If a GGN has disappeared, or decreased in size or density on follow-up CT, there is a chance that it was a focal infection and not cancer. Conversely, if a GGN is stable, growing, or becoming more solid, further examination is required to exclude malignancy (2,15). In this study, 37.1% of the cases showed a progressive change during follow-up beyond six months, which led to unnecessary surgical excision. Thus, understanding of GGNs is lacking. The differential diagnosis of GGNs with progressive changes is of great significance; however, currently, there is no relevant report on them.

VDT can be used for differential diagnosis and subsequent management. The VDT of growing malignant GGNs is usually >2 years, but it varies among the different types. The VDT of pGGNs and PSNs are 813 and 457 days, respectively (19,22). Thus, if the nodule is growing at a pace consistent with malignancy, it may be malignant and further evaluation is needed. If the nodule grows very slowly, an indolent malignancy remains possible (23). Conversely, if the nodule grows quickly, it is more likely to be an infectious lesion (24). Among the 28 lesions with increasing volume, most (71.4%) had a VDT <344 days, which was significantly shorter than that of the neoplastic pGGNs or PSNs. This difference could be a valuable clue for differential diagnosis. Additionally, the VDT of the GGNs with progressive changes exhibited significant variation, and their pathological findings were

8476

Jiang et al. CT features of progressive non-neoplastic GGNs

Table 4 Pathological characteristics of the GGNs with different types of progressive changes

Pathological results	Fibrous tissue proliferation with inflammatory cell infiltration	Fibrous tissue proliferation without inflammatory cell infiltration	P value
GGNs with no changes (n=35)	25 (71.4)	10 (28.6)	0.79[†]
GGNs with progressive changes (n=35)	26 (74.3)	9 (25.7)	
Type I (n=5)	3 (60.0)	2 (40.0)	
Type II (n=14)	12 (85.7)	2 (14.3)	
Type III (n=2)	2 (100)	0	
Type IV (n=9)	5 (55.6)	4 (44.4)	
Type V (n=5)	4 (80.0)	1 (20.0)	

Data are presented as n (%). [†], calculated with the Pearson Chi-squared test. GGNs, ground-glass nodules.

similar to those of the GGNs with no significant changes >6 months, which indicates that these lesions did not truly grow, or the inflammation in them continuously progressed, causing the GGNs to transiently expand before this follow-up, but the changes were not detected in time, resulting in an increase in the follow-up interval and VDT.

Other than the VDT, the period of changes in CT features is also important for differentiating between GGNs. GGNs that show significant changes in the short term may be benign (25). In this study, 11 cases showed significant changes within 3 months, indicating their nature as benign lesions. Conversely, the nodules that changed slowly were more difficultly to differentiate. Previous studies have confirmed that benign GGNs are usually ill-defined, while malignant GGNs typically have well-defined boundaries (11,26-29). In the current study, the boundaries of most of the GGNs were also ill-defined on both the initial and subsequent CT images, which is consistent with previous findings (11,26-29). However, the transition of the pathological components and density difference in the lesion-lung boundary zone of the GGNs may affect the visual illustration of their boundary (25). Nodules with more inflammatory cells are more likely to exhibit high density and ill-defined boundaries due to inflammatory cell infiltration and exudation; thus, an increase in density in GGNs is likely due to the progression of inflammation. Conversely, based on the main pathological findings, a well-defined boundary usually indicates an advanced stage of inflammation (25). Thus, rapid changes in CT features and an ill-defined boundary could serve as key features for identifying non-neoplastic GGNs with progressive changes during follow-up.

This study had several limitations. First, while it was a two-center study, the sample size was still very small, as most patients had no follow-up data and only patients who underwent GGN resection were enrolled in this study. Second, as this was a retrospective study, the follow-up intervals for the nodules varied. Third, as some patients were not scanned using the same CT scanner during follow-up, there was a risk that the evaluation of the density change was inaccurate; thus, only when the density of the GGNs increased by 100 HU was considered an increase in density. Fourth, the follow-up interval and boundary of lesions are helpful for the diagnosis of progressive non-neoplastic GGNs, but difficulties remain in diagnosing those without such relevant characteristics. Fifth, as the sample size of non-neoplastic GGNs with progressive changes was small, and there was a significant variation in the follow-up intervals, no comparison was made between non-neoplastic and neoplastic GGNs in this study. Therefore, further research on the differential diagnosis of non-neoplastic GGNs with progressive changes and neoplastic GGNs with a large sample is needed.

Conclusions

Among GGNs that show an increase in the size, density, or solid component during follow-up, a few cases may be non-neoplastic lesions. The development stage and follow-up interval of lesions may be related to their varied progressive changes. For further differential diagnosis, close attention should be paid to the follow-up interval, VDT and boundary of the GGNs with progressive changes. GGNs that change significantly in a short period or have ill-defined boundary both on initial and follow-up CT images should be highly suspected as non-neoplastic lesions.

Acknowledgments

Footnote

Reporting Checklist: The authors have completed the STROBE reporting checklist. Available at https://qims.amegroups.com/article/view/10.21037/qims-24-389/rc

Conflicts of Interest: All authors have completed the ICMJE uniform disclosure form (available at https://qims.amegroups.com/article/view/10.21037/qims-24-389/coif). The authors have no conflicts of interest to declare.

Ethical Statement: The authors are accountable for all aspects of the work in ensuring that questions related to the accuracy or integrity of any part of the work are appropriately investigated and resolved. The study was conducted in accordance with the Declaration of Helsinki (as revised in 2013), and the study protocol was approved by the Ethics Committees of The First Affiliated Hospital of Chongqing Medical University (No. 2019-062) and The Second Affiliated Hospital of Army Medical University (No. 2020-research147-01), and the requirement of written informed consent was waived due to the retrospective nature of the study.

References

1. Walter JE, Heuvelmans MA, de Bock GH, Yousaf-Khan U, Groen HJM, van der Aalst CM, Nackaerts K, van Ooijen PMA, de Koning HJ, Vliegenthart R, Oudkerk M. Relationship between the number of new nodules and lung cancer probability in incidence screening rounds of CT lung cancer screening: The NELSON study. Lung Cancer 2018;125:103-8.

2. MacMahon H, Naidich DP, Goo JM, Lee KS, Leung ANC, Mayo JR, Mehta AC, Ohno Y, Powell CA, Prokop M, Rubin GD, Schaefer-Prokop CM, Travis WD, Van Schil PE, Bankier AA. Guidelines for Management of Incidental Pulmonary Nodules Detected on CT Images: From the Fleischner Society 2017. Radiology 2017;284:228-43.

3. Gao F, Sun Y, Zhang G, Zheng X, Li M, Hua Y. CT characterization of different pathological types of subcentimeter pulmonary ground-glass nodular lesions. Br J Radiol 2019;92:20180204.

4. Hu X, Ye W, Li Z, Chen C, Cheng S, Lv X, Weng W, Li J, Weng Q, Pang P, Xu M, Chen M, Ji J. Non-invasive evaluation for benign and malignant subcentimeter pulmonary ground-glass nodules (≤1 cm) based on CT texture analysis. Br J Radiol 2020;93:20190762.

5. Sato Y, Fujimoto D, Morimoto T, Uehara K, Nagata K, Sakanoue I, Hamakawa H, Takahashi Y, Imai Y, Tomii K. Natural history and clinical characteristics of multiple pulmonary nodules with ground glass opacity. Respirology 2017;22:1615-21.

6. Zhang Z, Zhou L, Min X, Li H, Qi Q, Sun C, Sun K, Yang F, Li X. Long-term follow-up of persistent pulmonary subsolid nodules: Natural course of pure, heterogeneous, and real part-solid ground-glass nodules. Thorac Cancer 2023;14:1059-70.

7. Fu BJ, Lv FJ, Li WJ, Lin RY, Zheng YN, Chu ZG. Significance of intra-nodular vessel sign in differentiating benign and malignant pulmonary ground-glass nodules. Insights Imaging 2021;12:65.

8. Li WJ, Lv FJ, Tan YW, Fu BJ, Chu ZG. Pulmonary Benign Ground-Glass Nodules: CT Features and Pathological Findings. Int J Gen Med 2021;14:581-90.

9. Wu L, Gao C, Kong N, Lou X, Xu M. The long-term course of subsolid nodules and predictors of interval growth on chest CT: a systematic review and meta-analysis. Eur Radiol 2023;33:2075-88.

10. Fang W, Zhang G, Yu Y, Chen H, Liu H. Identification of pathological subtypes of early lung adenocarcinoma based on artificial intelligence parameters and CT signs. Biosci Rep 2022;42:BSR20212416.

11. He XQ, Li X, Wu Y, Wu S, Luo TY, Lv FJ, Li Q. Differential Diagnosis of Nonabsorbable Inflammatory and Malignant Subsolid Nodules with a Solid Component ≤5 mm. J Inflamm Res 2022;15:1785-96.

8478

Jiang et al. CT features of progressive non-neoplastic GGNs

12. He W, Guo G, Du X, Guo S, Zhuang X. CT imaging indications correlate with the degree of lung adenocarcinoma infiltration. Front Oncol 2023;13:1108758.

13. Shen C, Wu Q, Xia Q, Cao C, Wang F, Li Z, Fan L. Establishment of a malignancy and benignancy prediction model of sub-centimeter pulmonary ground-glass nodules based on the inflammation-cancer transformation theory. Front Med (Lausanne) 2022;9:1007589.

14. Alpert JB, Ko JP. Management of Incidental Lung Nodules: Current Strategy and Rationale. Radiol Clin North Am 2018;56:339-51.

15. National Comprehensive Cancer Network. NCCN Guidelines for Patients® Early and Locally Advanced Non-Small Cell Lung Cancer, Version 2023. Available online: https://www.nccn.org/patients/guidelines/content/PDF/lung-early-stage-patient.pdf

16. Kim YT. Management of Ground-Glass Nodules: When and How to Operate? Cancers (Basel) 2022;14:715.

17. Hansell DM, Bankier AA, MacMahon H, McLoud TC, Müller NL, Remy J. Fleischner Society: glossary of terms for thoracic imaging. Radiology 2008;246:697-722.

18. Kakinuma R, Noguchi M, Ashizawa K, Kuriyama K, Maeshima AM, Koizumi N, Kondo T, Matsuguma H, Nitta N, Ohmatsu H, Okami J, Suehisa H, Yamaji T, Kodama K, Mori K, Yamada K, Matsuno Y, Murayama S, Murata K. Natural History of Pulmonary Subsolid Nodules: A Prospective Multicenter Study. J Thorac Oncol 2016;11:1012-28.

19. Byrne SC, Hammer MM. Malignant Nodules Detected on Lung Cancer Screening CT: Yield of Short-Term Follow-Up CT in Showing Nodule Growth. AJR Am J Roentgenol 2022;219:735-41.

20. Li M, Zhu L, Lv Y, Shen L, Han Y, Ye B. Thin-slice computed tomography enables to classify pulmonary subsolid nodules into pre-invasive lesion/minimally invasive adenocarcinoma and invasive adenocarcinoma: a retrospective study. Sci Rep 2023;13:6999.

21. Hasegawa M, Sone S, Takashima S, Li F, Yang ZG, Maruyama Y, Watanabe T. Growth rate of small lung cancers detected on mass CT screening. Br J Radiol 2000;73:1252-9.

22. Patel VK, Naik SK, Naidich DP, Travis WD, Weingarten JA, Lazzaro R, Gutterman DD, Wentowski C, Grosu HB, Raoof S. A practical algorithmic approach to the diagnosis and management of solitary pulmonary nodules: part 1: radiologic characteristics and imaging modalities. Chest 2013;143:825-39.

23. Mazzone PJ, Lam L. Evaluating the Patient With a Pulmonary Nodule: A Review. JAMA 2022;327:264-73.

24. Soubani AO. The evaluation and management of the solitary pulmonary nodule. Postgrad Med J 2008;84:459-66.

25. Liu XL, Lv FJ, Fu BJ, Lin RY, Li WJ, Chu ZG. Correlations Between Inflammatory Cell Infiltration and Relative Density and the Boundary Manifestation of Pulmonary Non-Neoplastic Ground Glass Nodules. J Inflamm Res 2023;16:1147-55.

26. Fu BJ, Zhang XC, Lv FJ, Chu ZG. Potential Role of Intrapulmonary Concomitant Lesions in Differentiating Non-Neoplastic and Neoplastic Ground Glass Nodules. J Inflamm Res 2023;16:6155-66.

27. Chu ZG, Li WJ, Fu BJ, Lv FJ. CT Characteristics for Predicting Invasiveness in Pulmonary Pure Ground-Glass Nodules. AJR Am J Roentgenol 2020;215:351-8.

28. Li WJ, Lv FJ, Tan YW, Fu BJ, Chu ZG. Benign and malignant pulmonary part-solid nodules: differentiation via thin-section computed tomography. Quant Imaging Med Surg 2022;12:699-710.

29. Liang ZR, Ye M, Lv FJ, Fu BJ, Lin RY, Li WJ, Chu ZG. Differential diagnosis of benign and malignant patchy ground-glass opacity by thin-section computed tomography. BMC Cancer 2022;22:1206.